

Mice lacking perforin have improved regeneration of the injured femoral nerve

<https://doi.org/10.4103/1673-5374.332152>

Date of submission: April 29, 2021

Date of decision: June 7, 2021

Date of acceptance: July 17, 2021

Date of web publication: January 7, 2022

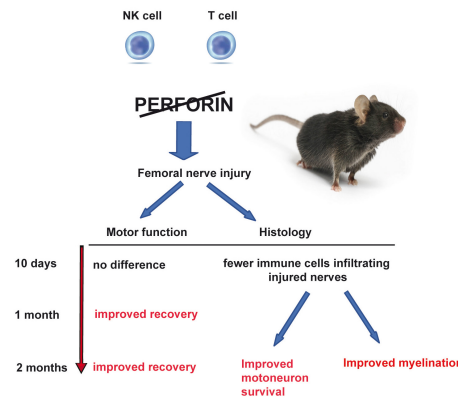
Igor Jakovčevski^{1,*}, Monika von Düring², David Lutz², Maja Vulović³,
Mohammad Hamad¹, Gebhard Reiss¹, Eckart Förster², Melitta Schachner^{4,*}

From the Contents

Introduction	1802
Materials and Methods	1803
Results	1805
Discussion	1805

Graphical Abstract

Effects of constitutive perforin ablation on motor recovery, myelination and motoneuron survival after femoral nerve injury in mice



Abstract

The role that the immune system plays after injury of the peripheral nervous system is still not completely understood. Perforin, a natural killer cell- and T-lymphocyte-derived enzyme that mediates cytotoxicity, plays important roles in autoimmune diseases, infections and central nervous system trauma, such as spinal cord injury. To dissect the roles of this single component of the immune response to injury, we tested regeneration after femoral nerve injury in perforin-deficient ($Pfp^{-/-}$) and wild-type control mice. Single frame motion analysis showed better motor recovery in $Pfp^{-/-}$ mice compared with control mice at 4 and 8 weeks after injury. Retrograde tracing of the motoneuron axons regrown into the motor nerve branch demonstrated more correctly projecting motoneurons in the spinal cord of $Pfp^{-/-}$ mice compared with wild-types. Myelination of regrown axons measured by g-ratio was more extensive in $Pfp^{-/-}$ than in wild-type mice in the motor branch of the femoral nerve. $Pfp^{-/-}$ mice displayed more cholinergic synaptic terminals around cell bodies of spinal motoneurons after injury than the injured wild-types. We histologically analyzed lymphocyte infiltration 10 days after surgery and found that in $Pfp^{-/-}$ mice the number of lymphocytes in the regenerating nerves was lower than in wild-types, suggesting a closed blood-nerve barrier in $Pfp^{-/-}$ mice. We conclude that perforin restricts motor recovery after femoral nerve injury owing to decreased survival of motoneurons and reduced myelination.

Key Words: blood-nerve barrier; femoral nerve injury; locomotor recovery; lymphocytes; myelination; NK-cells; perforin; reinnervation

Introduction

Abundance of conductive molecules and lack of growth inhibiting molecules in the peripheral nervous system allow regenerative processes to be more efficient than in the central nervous system (Irintchev, 2011; Divac et al., 2021). Despite this regenerative capacity, functional recovery upon peripheral nerve injury is often poor in patients and experimental animal models (Fu and Gordon, 1997; Irintchev and Schachner, 2012). The immune system plays important roles in peripheral nerve regeneration through opposing effects. On the one hand, the response of inflammatory cells to injury is an important defense mechanism, while on the other inflammatory cells produce potentially toxic cytokines that lead to exacerbation of tissue damage. For example, in mice with severe combined immunodeficiency, motor neurons survived poorly after facial nerve

transection (Serpe et al., 1999). Also, immune-deficient mice recover slower after facial nerve injury (Beahrs et al., 2010). In another study, autoimmune responses worsened the loss of motoneurons and exacerbated functional recovery after transection injury to the facial nerve (Ankeny and Popovich, 2007). Our previous work has indicated that mice constitutively deficient in the recombination activating gene 2 ($Rag2^{-/-}$) and therefore lacking functional T- and B-cells recover better after femoral nerve injury than the injured wild-type controls (Mehanna et al., 2014).

Similar to the central nervous system, the peripheral nervous system is immune-privileged owing to particular blood vessels of the “blood-nerve barrier” (Choi and Kim, 2008). Upon nerve injury, this barrier is opened and inflammatory and immune cells comprising macrophages, neutrophils and lymphocytes penetrate within hours

¹Institut für Anatomie und Klinische Morphologie, Universität Witten/Herdecke, Witten, Germany; ²Department of Neuroanatomy and Molecular Brain Research, Ruhr University Bochum, Bochum, Germany; ³Department of Anatomy, Faculty of Medical Sciences, University of Kragujevac, Kragujevac, Serbia;

⁴Keck Center for Collaborative Neuroscience and Department of Cell Biology and Neuroscience, Rutgers University, Piscataway, NJ, USA

*Correspondence to: Melitta Schachner, PhD, schachner@dls.rutgers.edu; Igor Jakovčevski, MD, Igor.Jakovcevski@uni-wh.de.

<https://orcid.org/0000-0002-3316-0778> (Melitta Schachner); <https://orcid.org/0000-0002-6654-8402> (Igor Jakovčevski)

Funding: This study was supported by the Li Kashing Foundation (to MS), the FoRUM grant F957N-2019 of the Ruhr-University Bochum (to DL), and the Heinrich und Alma Vogelsang Stiftung (to II).

How to cite this article: Jakovčevski I, von Düring M, Lutz D, Vulović M, Hamad M, Reiss G, Förster E, Schachner M (2022) Mice lacking perforin have improved regeneration of the injured femoral nerve. *Neural Regen Res* 17(8):1802-1808.

into the tissue at the site of injury, particularly into the proximal and distal stumps of the injured nerve which are undergoing degenerative processes – Wallerian degeneration of the distal stump and the retrograde degeneration of the proximal stump (Mignini et al., 2012; Napoli et al., 2012; Schmid et al., 2013).

Perforin is an important component of the immune system as natural killer (NK) and cytotoxic T-lymphocytes expressing perforin use this protein for pore formation of the plasma membrane of target cells, thus mediating cytotoxicity (Henkart, 1985; Liu et al., 1995; Voskoboinik et al., 2015). Moreover, perforin damages neurites *in vitro* (Miller et al., 2013) and contributes to neuronal degeneration in mouse models of multiple sclerosis (Deb et al., 2009, 2010; Hao et al., 2010), Parkinson's disease (Peng et al., 2017), stroke (Mracsko et al., 2014) and spinal cord injury (Liu et al., 2019; Jakovcevski and Schachner, 2020). Also, perforin causes blood-brain barrier disruption, which could contribute to immune cell infiltration and increased inflammatory damage as shown in different nervous system disorders (Suidan et al., 2008; Johnson et al., 2014; Willenbring et al., 2016; Huggins et al., 2017). It should be, however, noted that blood-nerve barrier is more readily disrupted by mechanical force as nerves are a highly vascular tissue, and so, upon injury, it is likely that the vascular system will feed into the neurodegenerative and regenerative responses.

Taken together, these findings raised the question whether deficiency in perforin would benefit regeneration after injury in the experimental model of femoral nerve transection. Using perforin deficient ($Pfp^{-/-}$) mice, we tested motor recovery, as well as histological parameters of regeneration upon injury. To our best knowledge, this is the first report that offers evidence for the role of perforin in peripheral nerve regeneration.

Materials and Methods

Animals

Seven wild-type C57BL/6NT mice and seven $Pfp^{-/-}$ mice were obtained from the breeding colony at the animal housing of the University Hospital Hamburg-Eppendorf. Mice were originally founded from a breeder line obtained from Taconic Farms Inc. and backcrossed twelve times into the C57BL/6NT background. Additionally, eight $Pfp^{+/+}$ and eight wild-type control mice backcrossed ten times into the C57BL/6J background were obtained from the Jackson Laboratory for histological analysis. Noteworthy, among these two slightly different mouse lines experimental outcomes were similar. All mice were male and entered the experiments at ages between 12 and 15 weeks (body weight 22–26 g). We used all male mice to avoid potential influence of the hormonal status on regeneration in female mice. Overall numbers of mice used for the experiments were 11 $Pfp^{-/-}$ and 11 wild-type control mice. Animals were kept single-caged in a specific pathogen-free facility under barrier conditions with filtered air flow, with 12-hour 7a.m. – 7p.m. light/dark cycle and controlled temperature of 21°C. Prior to injury all animals were inspected for overall behavioural abnormalities. All experiments were performed in accordance with the German laws on the protection of experimental animals, and all procedures were approved by the Department for Health and Consumer Protection of the State of Hamburg (project G09/098) and Department for Nature, Environment and Consumer Protection North Rhine-Westphalia (project 2019A.308). All experiments, collection of data and data analyses were performed by an experimenter blinded to genotypes and treatments.

Femoral nerve transection and reconstruction

Nerve transection and reconstruction were performed with special attention to keeping mice pathogen free (Mehanna et al., 2014). In brief, animals were anaesthetized by intraperitoneal injections of 0.4 mg/kg fentanyl (Fentanyl-Janssen, Janssen-Cilag GmbH, Neuss, Germany; product number N01AH01), 10 mg/kg droperidol (Xomolix, ProStrakan, Chambray-lès-Tours, France; product number N05AD08) and 5 mg/kg diazepam (Ratiopharm, Ulm, Germany). After exposing the right femoral nerve, nerve was transected 3 mm proximal to its bifurcation into mixed motor-sensory (quadriceps) and sensory (saphenous nerve) branches, and a 3-mm-long polyethylene tube of 0.58 mm inner diameter (Becton Dickinson, Heidelberg, Germany; product number 280410) was placed between the proximal and distal nerve stumps, filled with phosphate buffered saline (PBS), pH 7.3, to facilitate regeneration. The proximal and distal nerve ends were fixed into the polyethylene tube with 11-0 nylon stitches through epineurium on both ends (Ethilon, Norderstedt, Germany; product

number D7811), so that a 2-mm gap remained between them. Finally, the muscles were pulled back over the nerve and the skin wound was closed with a 6-0 suture (Ethicon). After surgery, mice received intraperitoneal injection of opiate buprenorphine (Temgesic, 0.05 mg/kg daily; Essex Pharma GmbH, Munich, Germany; product number 00345928) for 2 days, as previously described (Jakovcevski et al., 2021).

Motoneuron retrograde labeling

Eight weeks after nerve transection, after taking the last video recording, the animals were anesthetized as described above for retrograde labeling of the regrown axons (Akyüz et al., 2013). The right femoral nerve was exposed, and pieces of parafilm (Pechiney Plastic Packaging, Chicago, IL, USA) were inserted underneath the nerve. The two nerve branches, the saphenous (containing sensory and visceral motor axons) and quadriceps (mixed motor and sensory branch) branches, were again transected, this time approximately 5 mm distally from the bifurcation. Fluorescent retrograde tracers in powder form were applied to the proximal nerve ends: fluoro-ruby (tetramethylrhodamine dextran, ThermoFisher Scientific, Waltham, MA, USA; product number D1818) to the saphenous branch (cutaneous sensory and visceromotor branch), and Fast Blue (Polysciences Europe, Hirschberg an der Bergstrasse, Germany; product number 73819-41-7) to the quadriceps (muscle) branch (mixed nerve containing both sensory and somatomotor axons). Thirty minutes after dye application, the wound was closed after rinsing the nerve stumps with PBS. This labeling procedure fluorescently stains all motoneurons in the lumbar spinal cord which have successfully regenerated their axons at least to the level of transection. Additionally, it allows differentiation between motoneurons with axons projecting into the quadriceps branch (blue), further labelled as “correctly” projecting, and those wrongly projecting, sending axons to the saphenous branch (red) or to both the saphenous and quadriceps branches (white, labeled simultaneously with both blue and red dye). As with the first surgery, mice received intraperitoneal injection of buprenorphine (0.05 mg/kg daily for 2 days). It should be taken into account that the surgery for retrograde labeling causes second injury to the regenerated nerve. However, our previous work has shown that secondary injury does not significantly affect myelination within 7 days after tracing (Guseva et al., 2009, 2011; Mehanna et al., 2009, 2014; Akyüz et al., 2013). Additionally, we controlled for the effect of secondary injury by using four more wild-type and $Pfp^{-/-}$ mice that were injured and then sacrificed without retrograde tracing 2 months after injury. In these mice, the difference in myelination of injured motor nerve branches was present to a similar degree as in mice which were retrogradely traced (data not shown).

Single frame motion analysis

To assess locomotor function after injury, single frame motion analysis was performed (Irintchev et al., 2005). In brief, mice were trained to walk without exploratory pauses on a horizontal wooden beam (1-m-long, 38-mm-wide) leading to their home cage, which they typically learn in two to three trials, as the home cage presented a strong stimulus for return. After the learning phase and prior to surgery, one beam walking trial was video recorded at the animal's rear view. For video recordings capturing we used a high-speed digital camera (A602fc, Basler, Ahrensburg, Germany), capable of taking 100 frames per second. Videos were subsequently transferred and stored on a personal computer in .avi format. Each animal was recorded again at 1, 2, 4, 6 and 8 weeks after nerve transection and repair surgery. The videos were analyzed to select frames in which the animals were captured in specific gait cycle phases, according to the criteria for measurements of locomotor functional parameters, the foot-base and heels-tail angles (Irintchev et al., 2005). The foot-base angle (FBA) was measured at toe-off position at which the sole of the injured foot was approximately perpendicular to the beam, while the sole on the non-injured side was almost parallel to the beam. The angle was formed by the line dividing the sole longitudinally into two symmetrical halves and the horizontal line of the beam surface (Figure 1A and B). The heels-tail angle (HTA) was formed by the imaginary lines which connected both heels with the urethra (Figure 1C and D). The gait phase at which this angle was measured was the mid-swing of the contralateral (non-injured) leg. Nerve injury induces changes in both FBA and HTA, which arose from altered bending of the knee joint, due to weakness of the quadriceps muscle. Angle measurements were done using Fiji/ImageJ freeware (NIH, Bethesda, MD, USA). Additionally, we assessed another parameter, the protraction length ratio (PLR), using the pencil

grabbing test. In this test, the mouse was held by the tail and could grasp a pencil with its forelimbs, which was a reflex reaction in mice. The hind limbs performed grasping movements, i.e. alternating limb flexion and extension, aiming to grab the pencil tip which was held by the front limbs. The protractions in intact animals were symmetrical (PLR \approx 1), whereas after injury, the limb on the injured side could not be completely extended (Irintchev et al., 2005), so that PLR was higher than 1.

The recovery index was an individual estimate of recovery for parameters described above, calculated as: $RI = [(X_{7+n} - X_7)/(X_0 - X_7)] \times 100$, where X represents measured parameter values (X_0 – before injury, X_7 – 7 days after injury and X_{7+n} – 7 + n days after injury), and expressed in percent. These values yielded a recovery index measured as the ratio of regain-of-function to loss-of-function upon injury. Calculation of the recovery index is important whenever a parameter is prone to individual variability due to body constitution and behavioural traits (Irintchev et al., 2005). Moreover, the recovery index allows a comprehensive comparison between different parameters of recovery within one study or between different studies performed independently in other laboratories. It should be noted that the single frame motion analysis was developed specifically to analyze motor recovery after femoral nerve injury, as proper methods for analysis of recovery were not available and the outcome of femoral nerve injury was quantified mainly by histological analysis (Irintchev, 2011). Our prior experience using this method gives us confidence in reliability and reproducibility of our measurements (Guseva et al., 2011, 2018; Akyüz et al., 2013; Mehanna et al., 2014).

Tissue preparation for histology

One week after retrograde labeling surgery, thus 9 weeks after femoral nerve injury, the mice were anesthetized with 5 μ L/g body weight of sodium pentobarbital (Narcoren[®], Merial, Hallbergmoos, Germany), injected intraperitoneally. After the depth of narcosis was confirmed, the chest was open and mice were transcardially perfused for 1 minute with PBS, followed by a 10 minutes perfusion with 4% formaldehyde in 0.1 M sodium cacodylate buffer, pH 7.3. The spinal cords and femoral nerves from both sides (injured and contralateral, non-injured) were removed and post-fixed overnight in the fixative used for perfusion at 4°C. The tissue was then cryoprotected by immersion in the solution containing 20% sucrose in 0.1 M cacodylate buffer, pH 7.3, for 2 days at 4°C. The tissue was frozen by 2 minutes immersion in 2-methylbutane (isopentane) pre-cooled to -80°C, and then kept frozen at -80°C until sectioning. The spinal cord segment containing lumbar intumescence was glued to a specimen holder using Tissue-Tek[®] (Sakura Finetek Europe, Zoeterwoude, The Netherlands; product number 12351753). Serial 25- μ m-thick transverse (horizontal) spinal cord sections were cut on a cryostat (Leica CM3050; Leica), collected on SuperFrost[®] Plus glass slides (ThermoFisher Scientific; product number 15438060) and after 1 hour air-drying stored at -20°C until further use. These sections were used for the quantification of retrogradely labeled motoneurons and for the analysis of synapses, upon immunohistochemical staining (see below). The nerve tissue samples (both injured and non-injured) were, after perfusion and dissection, post-fixed in the solution containing 1% osmium tetroxide (Polysciences Europe, Eppelheim, Germany; product number 20816-12-0) dissolved in 0.1 M sodium cacodylate buffer, pH 7.3, for 1 hour at room temperature, dehydrated in a series of alcohols and embedded in resin. One micrometer-thick (“semithin”) cross-sections or longitudinal sections from the quadriceps (“motor”) and saphenous (“sensory”) nerve branches were cut, starting approximately 3 mm distally to the bifurcation. The sections were stained with the 1% toluidine blue and 1% borax in water and used for analysis of axon numbers, myelination and immune cell infiltration into the regenerated nerve tissue (Guseva et al., 2011; Mehanna et al., 2014).

Immunohistochemistry

To assess synaptic remodelling of retrogradely labelled motoneurons after injury, immunohistochemistry was performed as described previously (Guseva et al., 2018), on 25 μ m-thick cryosections. Sections were air-dried at 37°C for 30 minutes and then incubated in 10 mM sodium citrate solution (pH 9.0, adjusted with 0.1 M NaOH) preheated to 70°C for 30 minutes. The sections were left to cool at room temperature for approximately 30 minutes. Afterwards, unspecific binding sites for the secondary antibody were blocked using PBS solution containing 5% normal goat or donkey serum (depending on the secondary antibody) 0.2% Triton X-100 for permeabilization (ThermoFisher Scientific; product number 28314),

and 0.02% sodium azide (Merck, Darmstadt, Germany; product number 1066880100) at room temperature for 1 hour. The slices were then incubated at 4°C for 3 days with primary antibody against goat choline-acetyl transferase (ChAT), for cholinergic synapses (1:100; Millipore; product number AB144P; RRID: AB_2079751), or anti-mouse vesicular inhibitory transmitter transporter (VGAT), for inhibitory synapses (1:1000; Synaptic Systems, Göttingen, Germany; product number 131011; RRID: AB_887872) diluted in PBS containing 0.5% lambda-carrageenan and 0.02% w/v sodium azide in PBS. The sections were washed 3 times in PBS for 15 minutes each, and then incubated with the Cy-2 coupled donkey anti-goat (ab6948, for ChAT) or goat anti-mouse (ab6944, for VGAT) secondary antibody from Dianova, Hamburg, Germany, diluted 1:200 in 0.5% PBS-carrageenan at room temperature for 2 hours. After a subsequent wash in PBS (3 \times 15 minutes), for the staining of cell nuclei bis-benzamide solution (Hoechst 33258 dye, 5 μ g/mL in PBS, Sigma, St. Louis, MO, USA; product number 911004-45-0) was used at room temperature for 10 minutes. The sections were washed once with distilled water, mounted with Fluoromount G (Southern Biotechnology Associates; Biozol, Eching, Germany; product number SBA-0100-01) and stored in the refrigerator until further use.

Quantitative analysis of retrogradely labeled motoneurons

Transverse section series of spinal cords were examined using a fluorescence microscope (Axiophot 2, Zeiss, Oberkochen, Germany). Each section on which retrogradely labeled motoneurons were present was examined under a 40 \times objective by focusing through the section thickness from the top towards the bottom. All retrogradely traced motoneurons, with the exception of those sharply focused at the top of sections, were counted, to avoid double counting of traced cells (Akyüz et al., 2013). Motoneurons labeled with blue dye only, i.e. those projecting to the quadriceps branch, were considered correctly projecting, whereas motoneurons labeled red, or white (overlap between red and blue) were considered to be incorrectly projecting, as they had sent axons through the saphenous branch.

Analysis of axonal diameter profiles and myelination in regenerated nerve branches

Numbers of myelinated axons per nerve cross-section were counted using a NeuroLucida software-controlled computer system (MicroBrightField Europe, Magdeburg, Germany) under an Axioskop microscope (Zeiss), 100 \times oil objective magnification (Guseva et al., 2011). The diameter of myelinated axons and total nerve fibers (axon + myelin sheath) were measured in each section at corresponding locations. For sampling, a 60- μ m-spaced square grid was projected into the visual field using the NeuroLucida software, with random reference point selection. In all myelinated axons touching or crossing the vertical grid lines, the longest diameter and the diameter perpendicular to the longest diameter of axon and total nerve fiber were measured, and the mean orthogonal diameter was calculated. The degree of myelination was expressed as the g-ratio, i.e. the ratio of axon to fiber diameter (lower values represent thicker myelin).

Photographic documentation

Microphotographs were taken on the Axiophot 2 microscope equipped with a digital camera using ZEN software (Zeiss). Electron micrographs were taken on an LVEM25 transmission electron microscope (DeLong America, Montreal, Canada). The images were processed with the Adobe Photoshop CS5 software package (Adobe Systems Inc., San Jose, CA, USA). Digital image processing was limited to brightness/contrast adjustments and crop function.

Statistical analysis

Statistical analyses were performed using the Sigma Plot 12 software (Systat Software GmbH; Erkrath, Germany). We determined sample size based on the previously published experiments in the field (e.g. Mehanna et al., 2014). Analysis of motor recovery over time, as assessed by the foot-base and heels-tail angles, as well as the protraction length ratio and recovery index, was carried out by the two-way analysis of variance (ANOVA) for repeated measures, using variables “time” and “genotype”, followed by Tukey’s *post hoc* test. Analyses of the precision of motor reinnervation, numbers of myelinated axons and synaptic coverage of motoneurons were performed by one-way ANOVA with Tukey’s *post hoc* test. Analysis of the distribution of g-ratios in myelinated axons was performed using Kolmogorov-Smirnov test. The mean value \pm standard error of the mean (SEM) was taken as the representative value for multiple measurements per animal. The difference between the groups was considered significant at levels below 5%.

Results

Improved recovery of motor function in injured Pfp^{-/-} mice

Motor function was assessed over a 2-month time using a video-based single frame motion analysis approach (Figure 1A–D; Irintchev et al., 2005). Prior to injury, the values of all followed motor function parameters between Pfp^{-/-} and control mice were comparable (Figure 1E–H), indicating that perforin deficiency does not affect locomotor parameters as assessed by beam walking nor knee extension as estimated by the pencil grab test. At 1 and 2 weeks after injury, there were no differences between Pfp^{-/-} and wild-type mice, indicating that the damage caused by nerve transection was similar in the genotypes (Figure 1E–H). Four weeks after nerve surgery, the foot-base angle (FBA) had lower values in Pfp^{-/-} than in wild-type mice, indicating a better locomotion at this time point. This was, however, not the case at 8 weeks after injury, when the values in wild-types approached those of Pfp^{-/-} mice (Figure 1E). The values of the heels-tail angle (HTA) were also higher in Pfp^{-/-} than in wild-type mice at 8 weeks after injury, indicating better recovery in the perforin-deficient group (Figure 1F). The limb protraction length ratio, estimated with the pencil grab test, was also better in Pfp^{-/-} than in wild-type mice at 4, but not at 8 weeks after injury (Figure 1G). In addition, we calculated stance recovery indices, which represent averaged FBA and HTA recovery indices. At both 4 and 8 weeks after surgery, the average recovery indices of injured Pfp^{-/-} mice were higher than those of wild-types (Figure 1H).

Improved axonal regrowth from motoneurons in Pfp^{-/-} mice

To analyze the cellular basis for improved motor recovery, motoneurons were retrogradely labeled. Retrograde labeling of motoneurons was performed on the same animals that had been analyzed for motor function recovery over an eight-week time span after injury (Figure 2A and B). The number of motoneurons that were retrogradely labeled through the quadriceps and saphenous branches, as well as those labeled through both branches, and the overall number of labeled motoneurons was lower in wild-type mice versus Pfp^{-/-} mice (Figure 2C). A fraction of the labeled motoneurons had in both genotypes projected wrongly into the saphenous branch, while the other labeled motoneurons had projected correctly into the quadriceps branch. A higher number of motoneurons had correctly regrown into the motor nerve branch in Pfp^{-/-} mice than in wild-type mice (+31%; Figure 2C).

Enhanced remyelination in Pfp^{-/-} mice

Numbers of axons and degree of myelination in non-injured and regenerated nerves were estimated in toluidine blue-stained semithin sections. The total numbers of myelinated axons in the motor branch of the non-injured femoral nerve were similar in both genotypes, whereas at 2 months after injury the total numbers of myelinated axons were reduced in both genotypes (Figure 3A–C). Notably, there was a tendency towards higher numbers of myelinated axons in Pfp^{-/-} mice, but without statistically significant difference (Figure 3C). Analysis of myelination, measured by g-ratio, revealed differences between the genotypes on the injured side, in regenerated nerves, indicating improved myelination in Pfp^{-/-} mice, in comparison with wild-type mice (Figure 4A–F). On the non-injured contralateral side, both genotypes showed a similar degree of myelination (Figure 4F).

Increased numbers of cholinergic synaptic terminals around cell bodies of motoneurons of Pfp^{-/-} mice

The number of synaptic terminals was determined from the immunostainings around motoneurons which were retrogradely labeled in the lumbar spinal cord, following procedures described (Guseva et al., 2018). Spinal cord sections of Pfp^{-/-} and control mice were stained with anti-ChAT (Figure 5A and B) and anti-VGAT (Figure 5C and D) antibodies to visualize perisomatic cholinergic and inhibitory synapses, respectively. The size of motoneuron cell bodies in Pfp^{-/-} and wild-type mice with or without injury was evaluated for motoneurons innervating the muscle branch, as detected by blue dye labeling. There was a tendency for larger cell bodies to be seen in the injured versus non-injured animals of both genotypes, but no significant differences were found between genotypes, neither for injured nor for non-injured animals (Figure 5E). Analysis of cholinergic (ChAT⁺) terminals at motoneuronal cell bodies showed reduced numbers after injury in both genotypes when compared to the corresponding non-injured groups, but this reduction was less prominent in Pfp^{-/-} than in wild-type mice (Figure 5A, B, and F). The density of inhibitory (VGAT⁺) terminals did not differ between genotypes without injury and showed a tendency to lower values

after injury, but with no significant differences between genotypes (Figure 5C, D, and G).

Decreased infiltration of immune cells into regenerated femoral nerves of Pfp^{-/-} mice

As perforin was previously implicated in opening the blood-brain and blood-spinal cord barriers (Huggins et al., 2017; Liu et al., 2019), we tried to estimate the infiltration of immune cells at the site of nerve injury, thus assessing the function of the blood-nerve barrier. Numbers of immune cells in regenerating femoral nerves were determined 10 days after transection with toluidine blue-stained semithin sections of the nerve within the polyethylene tube. At this stage after injury, cell debris, regenerating axons and newly formed blood vessels were seen (Figure 6). Lymphocytes were found in blood vessels and in damaged tissue (Figure 6). In injured Pfp^{-/-} nerves, only a few lymphocytes were seen outside of blood vessels (Figure 6B and D), whereas in wild-type nerves lymphocytes were more abundant (Figure 6A and C).

Discussion

Here we show that recovery after femoral nerve injury is substantially better in perforin-deficient mice than in wild-type controls, signifying a negative influence of perforin on recovery. In addition, perforin deficiency is associated with better remyelination of motor axons, better motoneuronal survival and a more precise motor neuron reinnervation. This negative effect of perforin after femoral nerve injury is not surprising, as it has been shown that in several nervous system disease models perforin-deficient mice show a better outcome (Deb et al., 2009; Mracsko et al., 2014; Peng et al., 2017; Liu et al., 2019). It had also been shown that perforin derived from NK-lymphocytes, CD8⁺ (cytotoxic) and CD4⁺ (“helper”) T-lymphocytes damages neurites *in vitro* (Miller et al., 2013). Negative effects of perforin *in vivo* may arise from its destructive impact on the blood-brain barrier and blood-spinal cord barrier, possibly allowing immune cell to infiltrate the diseased tissue and increase inflammatory damage in central nervous system disorders (Suidan et al., 2008; Johnson et al., 2014). Furthermore, lytic granules containing perforin and serine proteases, called granzymes, may affect target cells in blood vessels and in nerves. The proposed mechanism of perforin action in axonal degeneration involves binding of NK cells to target axons forming the “immune synapse”, whereby granzymes penetrate the axonal intracellular space (Davies et al., 2020). It has been reported that granzyme B protease activity, which is independent of perforin protease activity, targets caspase 3, but it is not known whether the apoptotic caspase pathway leads to axonal degeneration. It is likely that granzymes might, in conjunction with perforin, affect nerve regeneration, therefore accounting for indirect effects of perforin ablation. Of note, calcium ion influx through the perforin-containing pores in the membrane destabilizes microtubules and leads to axon degeneration (Davies et al., 2020).

It has been suggested that peripheral nerves are immune-privileged as seen in the central nervous system (Jakovcevski et al., 2013; Neal and Gasque, 2016). The blood-nerve barrier consists predominantly of endothelial cells connected by tight junctions to form a non-permeable barrier, analogous to the blood-brain barrier in the central nervous system (Peltonen et al., 2013; Ubogu, 2015). The endoneurium behind the blood-nerve barrier contains Schwann cells, mast cells, macrophages and fibroblasts, all of which secrete a range of trophic factors important for axonal regrowth and Schwann cell proliferation, both of which are important for axonal regrowth and remyelination (Heumann et al., 1987). Macrophages have been proposed to be beneficial in clearing the debris after peripheral nerve injury, by infiltrating the distal nerve segment (Zigmond and Echevarria, 2019). The infiltration of macrophages has, however, been also associated with neuropathic pain, which additionally may be detrimental for recovery (Penas and Navarro, 2018). In addition to macrophages, NK cells have been implicated in chronic pain (Davies et al., 2020). Also, perforin-containing NK cells target sensory axons which mediate neurotoxicity through perforin’s pore-forming function causing calcium influx, leading to chronic pain (Davies et al., 2019). Results from our experiments do not show evidence for chronic pain (self-mutilation, lack of grooming, non-reactiveness to stimuli) in any group of animals. Yet, we cannot exclude the possibility that in addition to its detrimental effect on motoneuronal axons, a sensory component could also contribute to a better recovery in perforin-deficient mice.

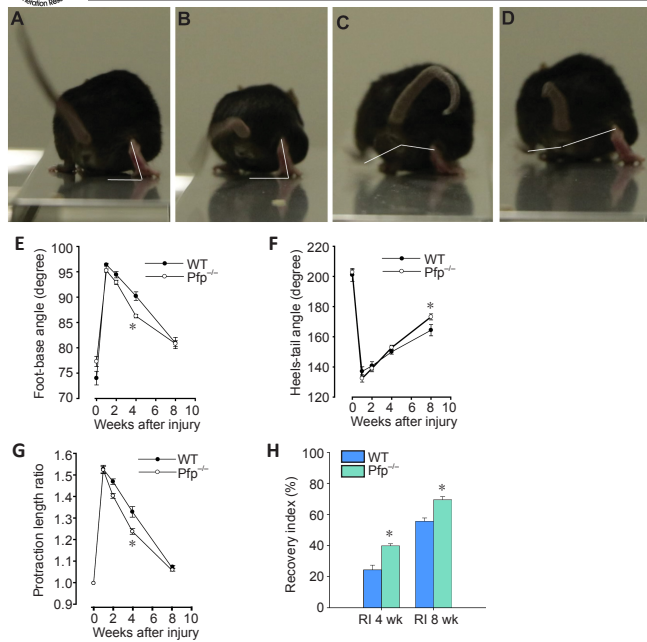


Figure 1 | Recovery parameters after femoral nerve injury. (A–D) Images represent foot-base angle (FBA; A, B) and heels-tail-angle (HTA; C, D) measurements in non-injured (A, C) and injured mice (B, D), 4 weeks after injury. Angles are depicted with white lines. (E–G) FBA (E), HTA (F) and protraction length ratios (G) in perforin-deficient ($Pfp^{-/-}$) mice and wild-type (WT) controls at different time-points after injury. Preoperative measures are shown as week 0. Data are shown as the mean \pm SEM. (H) Comparison of overall motor recovery in $Pfp^{-/-}$ and WT mice 4 weeks (wk) and 8 wk after injury. Bars represent the mean values \pm SEM of the stance recovery index (the mean value of the individual recovery index for HTA and FBA). * $P < 0.05$, vs. WT mice (two-way analysis of variance for repeated measures with Tukey's *post hoc* test). $n = 7$ mice per group.

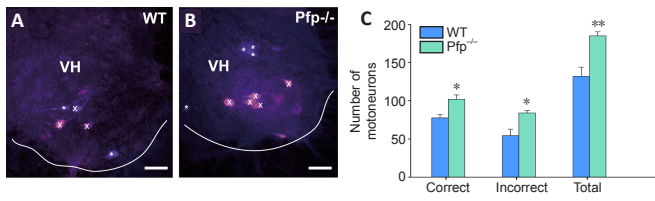


Figure 2 | Precision of motoneuron reinnervation after femoral nerve injury. Representative images of wild-type (WT, A) and perforin-deficient ($Pfp^{-/-}$) (B) ventral horns (VH) containing motoneurons retrogradely labeled through the quadriceps branch with Fast Blue (blue) and through the saphenous branch with Fluoro-ruby (red). White line demarcates spinal cord gray matter from white matter, asterisks label correctly projecting, and "x" signs incorrectly projecting motoneurons. Scale bars: 50 μ m. (C) The numbers of motoneurons labeled through the motor branch (correctly projecting 'correct'), the sensory branch (incorrectly projecting 'incorrect'), and the sum of correctly and incorrectly projecting neurons (total number, 'total') in wild-type (WT) and $Pfp^{-/-}$ mice 2 months after injury. Data are shown as the mean \pm SEM. * $P < 0.05$, ** $P < 0.01$, vs. WT mice (one-way analysis of variance with Tukey's *post hoc* test). $n = 6$ mice/group.

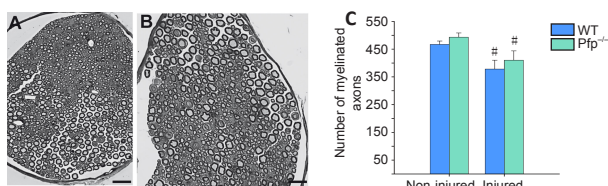


Figure 3 | Number of myelinated nerve fibers in injured and non-injured motor nerves. (A, B) Representative images of the injured quadriceps branches of wild-type (WT, A) and perforin-deficient ($Pfp^{-/-}$) mice (B). Scale bars: 20 μ m. (C) The number of myelinated axons in the motor (quadriceps) branch of WT and $Pfp^{-/-}$ mice, on the contralateral (non-injured) side and 2 months after injury (injured). Data are shown as the mean \pm SEM. # $P < 0.05$, vs. non-injured (contralateral) nerves (one-way analysis of variance with Tukey's *post hoc* test). $n = 6$ nerves/group.

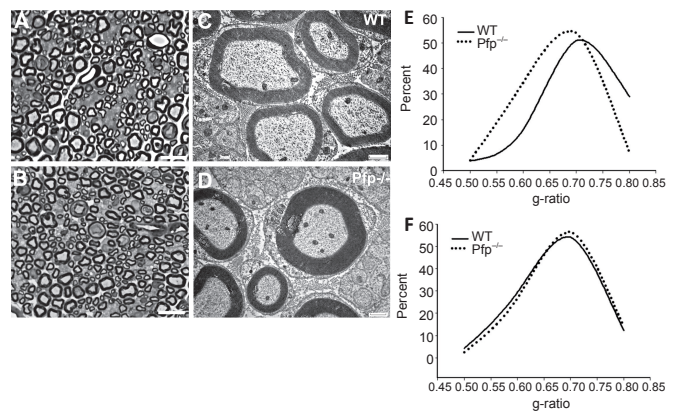


Figure 4 | Myelinated nerve fibers in motor nerve branches. Representative images show myelin on axons in the motor branch of wild-type (WT; A, C) and perforin-deficient ($Pfp^{-/-}$) (B, D) mice. A, B show light microscopy images, while C, D are transmission electron micrographs to demonstrate the quality of myelin fixation. Scale bars: 10 μ m in A, B and 500 nm in C, D. (E) Normalized frequency distributions for g-ratios (axon/fiber diameters) of the injured femoral nerve of WT and $Pfp^{-/-}$ mice, at 2 months after injury. Per nerve 75 axons were analyzed, from 6 nerves per genotype. The distribution in $Pfp^{-/-}$ nerves is different from the distribution of the WT group ($P < 0.001$, Kolmogorov-Smirnov test). (F) Normalized frequency distributions of g-ratios of the non-injured (contralateral) femoral nerve of WT and $Pfp^{-/-}$ mice. There is no difference between the distributions of g-ratios in non-injured nerves ($P > 0.05$, Kolmogorov-Smirnov test).

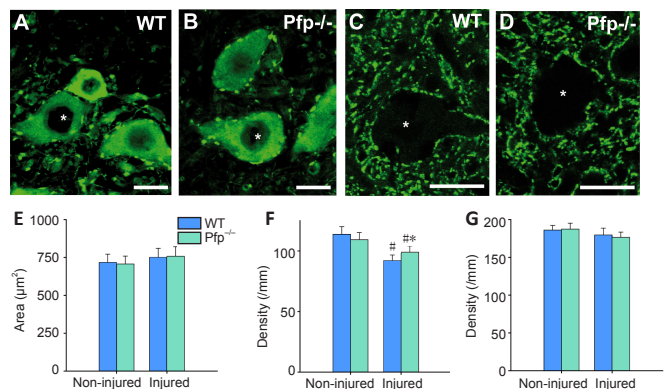


Figure 5 | Soma size of motoneurons and nerve terminals around retrogradely labeled motoneurons. Representative images of choline-acetyl transferase (ChAT) (A, B, green) and vesicular inhibitory transmitter transporter (VGAT) (C, D, green) immunostained motoneurons of perforin-deficient ($Pfp^{-/-}$) (B, D) and wild-type (WT; A, C) mice, 2 months after injury. Asterisks mark retrogradely labeled motoneurons which were analyzed. Scale bars: 15 μ m. Cell body area (E) and linear densities (number of puncta per mm) of ChAT⁺ (F) and VGAT⁺ (G) perisomatic terminals in non-injured and injured motoneurons, 2 months after injury. Graphs represent group mean values \pm SEM calculated from > 300 cells taken from 6 animals per group. * $P < 0.05$, vs. WT mice; # $P < 0.05$, vs. non-injured (one-way analysis of variance with Tukey's *post hoc* test).

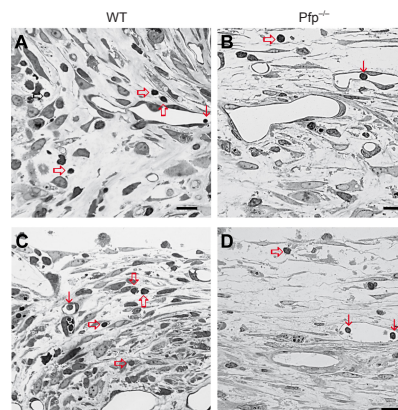


Figure 6 | Analysis of immune cells in regenerating femoral nerve tissue. Shown are representative images of toluidine-blue stained semithin sections of wild-type (WT) (A, C) and perforin-deficient ($Pfp^{-/-}$) (B, D) nerves 10 days after injury. Large arrows point to infiltrated lymphocytes. Thin arrows point to intravascular lymphocytes. Shown are representative images of 4 $Pfp^{-/-}$ and 4 WT mice. Scale bars: 10 μ m.

Schwann cells have been proposed to be part of the innate immune system, as they secrete different cytokines, including pro-inflammatory cytokines such as interleukin (IL)-1 β , IL-1 α , and IL-6, but also the anti-inflammatory cytokines such as tumor growth factor β and IL-10 (Martini and Willison, 2016). Also, Schwann cells may present antigens to infiltrating T-lymphocytes upon inflammatory stimulation, thus linking innate and adoptive immune systems (Meyer et al., 2010). It is, therefore, not unexpected that altered functions of perforin-deficient NK cells and T-cells are prone to occlude the blood-nerve barrier, thereby enabling better re-myelination. Indeed, judging by g-ratios, the quality of re-myelination in the motor branch of Pfp^{-/-} mice, 2 months after injury, is very similar to that of the non-injured nerve. Since Schwann cells also express perforin (Bonetti et al., 2003), it is plausible that perforin contributes to Schwann cell death.

Our study does not address the question of the cellular source of perforin in peripheral nerve injury. Of note, mice doubly deficient in perforin and Rag2 are incapable to generate an immune response and motoneurons survive poorly upon facial nerve injury (Byram et al., 2003). When in these mice NK cells were reconstituted, no effect on motoneuronal survival was observed, thus leading the authors to conclude that NK cells do not contribute to motoneuron survival after facial nerve injury (Byram et al., 2003). Thus, we would like to infer for our study that T-lymphocytes are the source of perforin, as described for spinal cord injury (Liu et al., 2019). Femoral nerve injury appears to be different from central nervous system injury with respect to motoneuronal survival, as in both Rag2- and perforin-deficient mice there are no adverse effects on motoneurons, and motor reinnervation is more precise (Mehanna et al., 2014).

Our findings on more precise motor reinnervation, better motoneuron survival and more perisomatic cholinergic synapses at the soma of motoneurons of Pfp^{-/-} mice compared with the controls are more difficult to explain. It is important to mention that the femoral nerve consists of a mainly sensory (saphenous) branch, which in addition contains visceromotor fibers, and a mixed motor-sensory (quadriceps) branch, which provides motor innervation for the femoral quadriceps muscle. Upon resection, motor axon therefore preferentially regrows through the quadriceps branch – a phenomenon called ‘preferential motor reinnervation’ (Brushart, 1988). Similar to Pfp^{-/-} mice, Rag2^{-/-} mice showed more precise motor reinnervation and better motoneuron survival (Mehanna et al., 2014), suggesting that the two mutants share a similar mechanism in recovery. As the common denominators in Rag2^{-/-} and Pfp^{-/-} mice are dysfunctional T-lymphocytes, we suggest that the combined adverse effects in perforin-expressing wild-type genotypes reduce motoneuron survival and precision of reinnervation after injury. The combined results indicate that T-lymphocytes are the predominant immune cell population relevant for perforin functions in the peripheral nervous system. T-lymphocytes have also been described to be important players in spinal cord injury (Liu et al., 2019). Of interest is the phenomenon of improved synaptic coverage of motoneurons in Pfp^{-/-} mice, signifying a central nervous system response to peripheral nerve injury (Vulovic et al., 2018). The number of cholinergic terminals at motoneuronal somata was lower in Rag2-deficient mice than in wild-types (Mehanna et al., 2014), whereas in Pfp^{-/-} mice this number is higher than in wild-type controls. This finding is the most conspicuous difference in the regenerative outcome after nerve injury between Rag2- and perforin-deficient mice. In agreement, the number of perisomatic cholinergic terminals was higher in perforin-deficient mice after spinal cord injury (Jakovcevski and Schachner, 2020). Ablation of perforin increases cholinergic synaptic coverage of motoneurons after injury which does not appear to be a developmental event, since in uninjured spinal cords no difference in synaptic coverage between the Pfp^{-/-} and wild-type mice was observed. It is noteworthy in this respect that spinal cord microglia, infiltrating macrophages and astrocytes play important roles in synaptic remodeling after injury (Irintchev et al., 2018; Vulovic et al., 2018; Jakovcevski et al., 2021). This remodeling takes place immediately after nerve injury when synaptic stripping occurs, which is reversed over time by synaptogenesis during muscle reinnervation (Hundeshagen et al., 2013; Raslan et al., 2014; Schultz et al., 2017). Thus, better axonal regeneration in Pfp^{-/-} mice could indirectly lead to enhanced synaptogenesis compared with wild-type mice. Alternatively, or additionally, we can speculate that nerve injury affects glial response within the spinal cord differently in Pfp^{-/-} and wild-type mice. In this context it is noteworthy that Pfp^{-/-} mice have decreased numbers of microglia/macrophages and astrocytes after spinal cord injury (Jakovcevski and Schachner, 2020).

Limitations

Our study is the first to show that in the absence of perforin, mice show improved regeneration after femoral nerve injury. Its main limitation is that the constitutional ablation of perforin could potentially cause developmental effects which result in better regeneration and may or may not be directly caused by perforin. The lack of measurable differences in contralateral nerves between Pfp^{-/-} and WT mice, as well as normal walking pattern in Pfp^{-/-} mice prior to injury suggest that this scenario is not very probable. However, a gain-of function study in Pfp^{-/-} mice, or conditional knockout in adult mice would give a definite answer.

Conclusion

We show that in the absence of perforin, mice have a better locomotor outcome two months after femoral nerve injury, as well as better outcomes in histological parameters – re-myelination, reinnervation precision and synaptic remodeling of motoneurons after injury. Our observations suggest that decreased permeability of the blood-nerve barrier and reduced perforin-mediated toxicity can at least partially explain these positive effects. Based on the dynamics of locomotor recovery in the absence of perforin, it appears that the role of perforin is most pronounced in the early phase after injury. It will be interesting to investigate if a perforin-targeting therapy, for example using topically delivered anti-perforin antibodies (Fujinaka et al., 2007) could have clinical significance.

Acknowledgments: We are very grateful to Emanuela Szpotowicz and Luzie Augustinowski for excellent technical assistance.

Author contributions: IJ and MS conceived the study. IJ, MvD, DL, MH and MV performed experiments and collected data. IJ, GR and EF designed experiments and analyzed data. IJ, DL, EF and MS analyzed data and wrote the manuscript. All authors approved the final manuscript version.

Conflicts of interest: The authors have no conflicts of interest to declare.

Editor note: MS is an Editorial Board member of Neural Regeneration Research. She was blinded from reviewing or making decisions on the manuscript. The article was subject to the journal's standard procedures, with peer review handled independently of this Editorial Board member and their research groups.

Open access statement: This is an open access journal, and articles are distributed under the terms of the Creative Commons Attribution Non-Commercial-ShareAlike 4.0 License, which allows others to remix, tweak, and build upon the work non-commercially, as long as appropriate credit is given and the new creations are licensed under the identical terms.

©Article author(s) (unless otherwise stated in the text of the article) 2022. All rights reserved. No commercial use is permitted unless otherwise expressly granted.

References

- Akyüz N, Rost S, Mehanna A, Bian S, Loers G, Oezen I, Mishra B, Hoffmann K, Guseva D, Laczynska E, Irintchev A, Jakovcevski I, Schachner M (2013) Dermatan 4-O-sulfotransferase1 ablation accelerates peripheral nerve regeneration. *Exp Neurol* 247:517-530.
- Ankeny DP, Popovich PG (2007) Central nervous system and non-central nervous system antigen vaccines exacerbate neuropathology caused by nerve injury. *Eur J Neurosci* 25:2053-2064.
- Beahrs T, Tanzer L, Sanders VM, Jones KJ (2010) Functional recovery and facial motoneuron survival are influenced by immunodeficiency in crush-axotomized mice. *Exp Neurol* 221:225-230.
- Bonetti B, Valdo P, Ossi G, De Toni L, Masotto B, Marconi S, Rizzuto N, Nardelli E, Moretto G (2003) T-cell cytotoxicity of human Schwann cells: TNF α promotes fasL-mediated apoptosis and IFN gamma perforin-mediated lysis. *Glia* 43:141-148.
- Brushart TM (1988) Preferential reinnervation of motor nerves by regenerating motor axons. *J Neurosci* 8:1026-1031.
- Byram SC, Serpe CJ, Pruet SB, Sanders VM, Jones KJ (2003) Natural killer cells do not mediate facial motoneuron survival after facial nerve transection. *Brain Behav Immun* 17:417-425.
- Choi YK, Kim KW (2008) Blood-neural barrier: its diversity and coordinated cell-to-cell communication. *BMB Rep* 41:345-352.
- Davies AJ, Kim HW, Gonzalez-Cano R, Choi J, Back SK, Roh SE, Johnson E, Gabriac M, Kim MS, Lee J, Lee JE, Kim YS, Bae YC, Kim SJ, Lee KM, Na HS, Riva P, Latremoliere A, Rinaldi S, Ugolini S, Costigan M, Oh SB (2019) Natural killer cells degenerate intact sensory afferents following nerve injury. *Cell* 176:716-728.

- Davies AJ, Rinaldi S, Costigan M, Oh SB (2020) Cytotoxic immunity in peripheral nerve injury and pain. *Front Neurosci* 14:142.
- Deb C, LaFrance-Corey RG, Zoelcklein L, Papke L, Rodriguez M, Howe CL (2009) Demyelinated axons and motor function are protected by genetic deletion of perforin in a mouse model of multiple sclerosis. *J Neuropathol Exp Neurol* 68:1037-1048.
- Deb C, LaFrance-Corey RG, Schmalstieg WF, Sauer BM, Wang H, German CL, Windebank AJ, Rodriguez M, Howe CL (2010) CD8+ T cells cause disability and axon loss in a mouse model of multiple sclerosis. *PLoS One* 5:e12478.
- Divac N, Aksić M, Rasulić L, Jakovčevski M, Basailović M, Jakovčevski I (2021) Pharmacology of repair after peripheral nerve injury. *Int J Clin Pharmacol Ther* 59:447-462.
- Fu SY, Gordon T (1997) The cellular and molecular basis of peripheral nerve regeneration. *Mol Neurobiol* 14:67-116.
- Fujinaka H, Yamamoto T, Feng L, Nameta M, Garcia G, Chen S, El-shemi AGA, Ohshiro K, Katsuyama K, Yoshida Y, Yaito E, Wilson CB (2007) Anti-perforin antibody treatment ameliorates experimental crescentic glomerulonephritis in WKY rats. *Kidney Int* 72:823-830.
- Guseva D, Angelov DN, Irintchev A, Schachner M (2009) Ablation of adhesion molecule L1 in mice favours Schwann cell proliferation and functional recovery after peripheral nerve injury. *Brain* 132:2180-2195.
- Guseva D, Zerwas M, Xiao MF, Jakovcevski I, Irintchev A, Schachner M (2011) Adhesion molecule L1 overexpressed under the control of the neuronal Thy-1 promoter improves myelination after peripheral nerve injury in adult mice. *Exp Neurol* 229:339-352.
- Guseva D, Jakovcevski I, Irintchev A, Leshchyn'ska I, Sytnyk V, Ponimaskin E, Schachner M (2018) Cell adhesion molecule close homolog of L1 (CHL1) guides the regrowth of regenerating motor axons and regulates synaptic coverage of motor neurons. *Front Mol Neurosci* 11:174.
- Hao J, Liu R, Piao W, Zhou Q, Vollmer TL, Campagnolo DI, Xiang R, La Cava A, Van Kaer L, Shi FD (2010) Central nervous system (CNS)-resident natural killer cells suppress Th17 responses and CNS autoimmune pathology. *J Exp Med* 207:1907-1921.
- Henkart PA (1985) Mechanism of lymphocyte-mediated cytotoxicity. *Ann Rev Immun* 3:31-58.
- Heumann R, Korsching S, Bandtlow C, Thoenen H (1987) Changes of nerve growth factor synthesis in non-neuronal cells in response to sciatic nerve transection. *J Cell Biol* 104:1623-1631.
- Huggins MA, Johnson HL, Jin F, N Songo A, Hanson LM, LaFrance SJ, Butler NS, Harty JT, Johnson AJ (2017) Perforin expression by CD8 T cells is sufficient to cause fatal brain edema during experimental cerebral malaria. *Infect Immun* 85:e00985-16.
- Hundeshagen G, Szameit K, Thieme H, Finkensieper M, Angelov DN, Guntinas-Lichius O, Irintchev A (2013) Deficient functional recovery after facial nerve crush in rats is associated with restricted rearrangements of synaptic terminals in the facial nucleus. *Neuroscience* 248:307-318.
- Irintchev A, Simova O, Eberhardt KA, Morellini F, Schachner M (2005) Impacts of lesion severity and tyrosine kinase receptor B deficiency on functional outcome of femoral nerve injury assessed by a novel single-frame motion analysis in mice. *Eur J Neurosci* 22:802-808.
- Irintchev A (2011) Potentials and limitations of peripheral nerve injury models in rodents with particular reference to the femoral nerve. *Ann Anat* 193:276-285.
- Irintchev A, Schachner M (2012) The injured and regenerating nervous system: immunoglobulin superfamily members as key players. *Neuroscientist* 18:452-466.
- Irintchev M, Guntinas-Lichius O, Irintchev A (2018) Botulinum neurotoxin application to the severed femoral nerve modulates spinal synaptic responses to axotomy and enhances motor recovery in rats. *Neural Plasticity* 2018:7975013.
- Jakovcevski I, Miljkovic D, Schachner M, Andjus PR (2013) Tenascins and inflammation in disorders of the nervous system. *Amino Acids* 44:1115-1127.
- Jakovcevski I, Schachner M (2020) Perforin affects regeneration in a mouse spinal cord injury model. *Int J Neurosci* doi: 10.1080/00207454.2020.1796662.
- Jakovcevski I, Förster E, Reiss G, Schachner M (2021) Impact of depletion of microglia/macrophages on regeneration after spinal cord injury. *Neuroscience* 459:129-141.
- Johnson HL, Willenbring RC, Jin F, Manhart WA, LaFrance SJ, Pirko I, Johnson AJ (2014) Perforin competent CD8 T cells are sufficient to cause immune-mediated blood-brain barrier disruption. *PLoS One* 9:e111401.
- Liu CC, Persechini PM, Young JD (1995) Perforin and lymphocyte-mediated cytotoxicity. *Immun Rev* 146:145-175.
- Liu Z, Zhang H, Xia H, Wang B, Zhang R, Zeng Q, Guo L, Shen K, Wang B, Zhong Y, Li Z, Sun G (2019) CD8 T cell-derived perforin aggravates secondary spinal cord injury through destroying the blood-spinal cord barrier. *Biochem Biophys Res Commun* 512:367-372.
- Martini R, Willison H (2016) Neuroinflammation in the peripheral nerve: Cause, modulator, or bystander in peripheral neuropathies? *Glia* 64:475-486.
- Mehanna A, Mishra B, Kurschat N, Schulze C, Bian S, Loers G, Irintchev A, Schachner M (2009) Polysialic acid glycomimetics promote myelination and functional recovery after peripheral injury in mice. *Brain* 132:1449-1462.
- Mehanna A, Szpotowicz E, Schachner M, Jakovcevski I (2014) Improved regeneration after femoral nerve injury in mice lacking functional T- and B-lymphocytes. *Exp Neurol* 261:147-155.
- Meyer G, Heidenreich H, Mausberg AK, Lehmann HC, ten Asbroek AL, Saavedra JT, Baas F, Hartung HP, Wiendl H, Kieseier BC (2010) Mouse Schwann cells activate MHC class I and II restricted T-cell responses, but require external peptide processing for MHC class II presentation. *Neurobiol Dis* 37:483-490.
- Mignini F, Giovannetti F, Cocchioni M, Ingrid R, Iannetti G (2012) Neuropeptide expression and T-lymphocyte recruitment in facial nucleus after facial nerve axotomy. *J Craniofac Surg* 23:1479-1483.
- Miller NM, Shriver LP, Bodiga VL, Ray A, Basu S, Ahuja R, Jana A, Pahan K, Ditte BN (2013) Lymphocytes with cytotoxic activity induce rapid microtubule axonal destabilization independently and before signs of neuronal death. *ASN Neuro* 5:e00105.
- Mracsko E, Liesz A, Stojanovic A, Lou WP, Osswald M, Zhou W, Karcher S, Winkler F, Martin-Villalba A, Cerwenka A, Veltkamp R (2014) Antigen dependently activated cluster of differentiation 8-positive T cells cause perforin-mediated neurotoxicity in experimental stroke. *J Neurosci* 34:16784-16795.
- Napoli I, Noon LA, Ribeiro S, Kerai AP, Parrinello S, Rosenberg LH, Collins MJ, Harrisingh MC, White IJ, Woodhoo A, Lloyd AC (2012) A central role for the ERK-signaling pathway in controlling Schwann cell plasticity and peripheral nerve regeneration in vivo. *Neuron* 73:729-742.
- Neal JW, Gasque P (2016) The role of primary infection of Schwann cells in the aetiology of infective inflammatory neuropathies. *J Infect* 73:402-418.
- Peltonen S, Alanne M, Peltonen J (2013) Barriers of the peripheral nerve. *Tissue Barriers* 1:3.
- Penas C, Navarro X (2018) Epigenetic modifications associated to neuroinflammation and neuropathic pain after neural trauma. *Front Cell Neurosci* 12:158.
- Peng SP, Zhang Y, Copray S, Schachner M, Shen YQ (2017) Participation of perforin in mediating dopaminergic neuron loss in MPTP-induced Parkinson's disease in mice. *Biochem Biophys Res Commun* 484:618-622.
- Raslan A, Ernst P, Werle M, Thieme H, Szameit K, Finkensieper M, Guntinas-Lichius O, Irintchev A (2014) Reduced cholinergic and glutamatergic synaptic input to regenerated motoneurons after facial nerve repair in rats: potential implications for recovery of motor function. *Brain Struct Funct* 219:891-909.
- Schmid AB, Coppieters MW, Ruitenber MJ, McLachlan EM (2013) Local and remote immune-mediated inflammation after mild peripheral nerve compression in rats. *J Neuropathol Exp Neurol* 72:662-680.
- Schultz AJ, Rotterman TM, Dwarakanath A, Alvarez FJ (2017) VGLUT1 synapses and P-boutons on regenerating motoneurons after nerve crush. *J Comp Neurol* 525:2876-2889.
- Serpe CJ, Kohm AP, Huppenbauer CB, Sanders VM, Jones KJ (1999) Exacerbation of facial motoneuron loss after facial nerve transection in severe combined immunodeficient (scid) mice. *J Neurosci* 19:RC7.
- Suidan GL, McDole JR, Chen Y, Pirko I, Johnson AJ (2008) Induction of blood brain barrier tight junction protein alterations by CD8 T cells. *PLoS One* 3:e3037.
- Ubogu EE (2015) Inflammatory neuropathies: pathology, molecular markers and targets for specific therapeutic intervention. *Acta Neuropath* 130:445-468.
- Voskoboinik I, Whisstock JC, Trapani JA (2015) Perforin and granzymes: function, dysfunction and human pathology. *Nat Rev Immun* 15:388-400.
- Vulovic M, Divac N, Jakovcevski I (2018) Confocal synaptology: synaptic rearrangements in neurodegenerative disorders and upon nervous system injury. *Front Neuroanat* 12:11.
- Willenbring RC, Jin F, Hinton DJ, Hansen M, Choi DS, Pavelko KD, Johnson AJ (2016) Modulatory effects of perforin gene dosage on pathogen-associated blood-brain barrier (BBB) disruption. *J Neuroinflammation* 13:222.
- Zigmond RE, Echevarria FD (2019) Macrophage biology in the peripheral nervous system after injury. *Prog Neurobiol* 173:102-121.

C-Editors: Zhao M, Zhao LJ, Li CH; T-Editor: Jia Y